Journal of Power Sources 269 (2014) 804–811

Contents lists available at ScienceDirect

Journal of Power Sources

journal homepage: www.elsevier.com/locate/jpowsour

Fire behavior of carbonates-based electrolytes used in Li-ion rechargeable batteries with a focus on the role of the $LiPF_6$ and LiFSI salts

Gebrekidan Gebresilassie Eshetu [a, b, c], Jean-Pierre Bertrand [a], Amandine Lecocq [a], Sylvie Grugeon [b, c], Stephane Laruelle [b, c], Michel Armand [b], Guy Marlair [a, *]

[a] Institut National de l'Environnement Industriel et des Risques (INERIS), Parc Technologique Alata, BP2, 60550 Verneuil-en-Halatte, France
[b] Laboratoire de Réactivité et de Chimie des Solides, UMR CNRS 7314, Université de Picardie Jules Verne, 33 rue Saint Leu, 80039 Amiens, France
[c] Réseau sur le Stockage Electrochimique de l'Energie (RS2E), FR CNRS 3459, France

HIGHLIGHTS

- Comparative fire behavior of $LiPF_6$ or LiFSI containing electrolytes was studied.
- Salt discriminating effect impacting overall related electrolyte pool burning mode.
- Effective heat of pool combustion were determined and ranged between 11 and 16 kJ g^{-1}.
- Fire toxicity bound to late production of irritants (HF, SO_2) and asphyxiants (CO).

ARTICLE INFO

Article history:
Received 5 May 2014
Received in revised form
19 June 2014
Accepted 9 July 2014
Available online 18 July 2014

Keywords:
Lithium-ion battery
Safety
LiFSI
Combustion
Electrolyte

ABSTRACT

A detailed investigation of the combustion behavior of $LiPF_6$ or LiFSI-based carbonate electrolytes was conducted with the objective of getting better knowledge of lithium-ion battery system fire induced thermal and chemical threats. The well–controlled experimental conditions provided by the Tewarson calorimeter have enabled the accurate evaluation of fire hazard rating parameters such as heat release rate and effective heat of combustion and the quantification of toxic effluents (HF, SO_2, NO_x…). Results have shown that all the electrolytes tested burn in phases depending on the flammability nature of their mixture constituents. The first stage of combustion is solely governed by the more volatile solvent (linear carbonate) and the influence of adding salt comes into effect predominantly in the second stage. It has been also shown that combustion enthalpy of electrolytes lies in the solvent mixture, irrespective of the salt added. The fire induced toxicity in well-ventilated conditions is found to be mainly dictated by the salt and its chemical structure, showing very limited concerns that emanate from the organic solvents.

1. Introduction

Owing to their success in the domain of hand-held devices, lithium-ion battery (LIB) is now being considered as the key technology for emerging innovative large-scale applications (automobile, solar and wind energy…) and grid storage (load leveling, integration of renewable energy sources etc…). The impetus behind the development of this technology is to reduce our dependence on depleting petroleum, trim down emission of greenhouse gases, mitigate global warming and thereby protect the environment. Over the past two decades, research development on LIB technology has markedly improved the electrochemical performances. Yet, the stringent safety requirements for such large-scale applications remain a major hurdle, slowing down their commercialization for the foreseen staggering energy storage demands.

Because of its contact with the strongly reducing anodes and oxidizing cathodes, and its flammable/combustible constituents, the electrolyte is considered as the most detrimental part of the LIB pertaining to both its thermal stability [1,2] and fire-induced risks [3,4]. When Li-ion batteries are under off-normal conditions either by electrical, mechanical, thermal or internal fault abuse events, electrolytes can be ejected into air, generally in the form of aerosols which can possibly ignite with air and resulting in fire and

* Corresponding author.
E-mail addresses: gly.marlair@free.fr, guy.marlair@ineris.fr (G. Marlair).

http://dx.doi.org/10.1016/j.jpowsour.2014.07.065
0378-7753/

explosion depending on local temperature, pressure, gas composition, etc… [5–13] The energy dissipated accidentally by a burning electrolyte is several times larger than the electrical energy stored in a battery and its accident scenario has some of the serious consequences, resulting in cascading failure of other cells in the battery assembly (module or pack) [14].

While a number of efforts are being devoted to qualifying the safety issues of LIBs, studies dealing with the fire-induced hazards of battery components are much scarcer [15]. Safety of large format Li-ion technology is a systemic issue with a number of inputs and factors and cannot be evaluated by a single criterion or simple set of parameters. Rather, it has to be determined by implementation of complementary approaches and the full safety appraisal of LIBs requires a systematic approach aiming at investigating at cell component, cell level, modules and packs. To address the aforementioned safety issues, our research group has started a step by step detailed evaluation of both the thermal [16,17] and chemical fire-induced hazards of classical liquid electrolytes used in state-of-the-art lithium-ion batteries. Their basic function is to serve as medium for the transfer of charges between the anode and the cathode. In practice, due to the diverse requirements of batteries such as wide functioning temperature ranges, power or energy demanding, most electrolyte formulations are based on solutions of blends of two or more solvents in which ~1 M lithium salts is dissolved. These blends are usually composed of flammable linear carbonates (dialkyl carbonates with alkyl = methyl and/or ethyl) and combustible cyclic carbonates solvents (e.g. ethylene and/or propylene carbonate). The idea is that the cyclic carbonates help to the lithium salt dissociation owing to their high dielectric constant and take on task to create the most part of the well-known passivation layer so called SEI (Solid Electrolyte Interphase) at the surface of the negative electrode active material preventing further detrimental electrolyte degradation while the low viscosity acyclic carbonates solvents assure good performances under low temperature environment.

The fire hazards were evaluated using the multi-purpose fire calorimeter, called Fire Propagation Apparatus or Tewarson calorimeter (over-instrumented version of ISO 12136). Following the previous studies devoted to analyzing the carbonate-based solvents fire behavior [18], in this paper, we propose a comparative study on the influence of the addition of the lithium salt (LiFSI [19–22] and $LiPF_6$) on fire parameters and gases release. $LiPF_6$, known to avoid aluminum collector corrosion is the classical salt used in the ~4 V functioning LIBs whereas $LiN(SO_2F)_2$ (called LiFSI), is entering the composition of liquid electrolytes in the $LiFePO_4$ (~3.5 V *vs.* Li^+/Li°) -based batteries to provide best low temperature performances. This paper is divided into two main parts. The first part is focused on the comparative thermal threat aspect of fires of $LiPF_6$ and LiFSI-based electrolytes (time to ignition (TTI), heat release rate (HRR), residue analysis, effective heat of combustion), and the second part deals with chemical threat aspect of fires of these electrolytes through a careful toxic gases yield analysis.

2. Experimental

Seven different $LiPF_6$-based formulations (Table 1), known as typical candidates for lithium-ion battery electrolytes, were investigated as received from Merck KGaA, Darmstadt, Germany. The LiFSI-based electrolyte (called LF100 in this study) has been prepared inside a dried glove box (O_2 and H_2O < 0.1 ppm) with the pure solvents (purity > 99.9%) also purchased from Merck supplier and a high quality of LiFSI salt obtained from Suzhou Fluolyte Co.Ltd.

The fire experiments were carried out by means of the fire propagation apparatus (ASTM E2058 and NFPA 287), also called the Tewarson apparatus [23–25]. It consists of a combustion region physically delimited by an infrared transparent quartz tube in which an incoming air flow of 350 and 80–30 L min^{-1} for oxygen rich and lean environments respectively was adjusted in order to simulate both under-ventilated and well-ventilated conditions.

Table 1
Designation and composition of $LiPF_6$ and LiFSI-based electrolytes.

Electrolyte designation	Corresponding solvent mixture	Nature of salt
LP30	EC/DMC (1/1, wt/wt)	$LiPF_6$ (11.8%,wt)
LP40	EC/DEC (1/1, wt/wt)	$LiPF_6$ (12.4%,wt)
LP47	EC/DEC (3/7, wt/wt)	$LiPF_6$ (13.1%,wt)
LP50	EC/EMC (1/1, wt/wt)	$LiPF_6$ (12.2%,wt)
LP57	EC/EMC (3/7, wt/wt)	$LiPF_6$ (12.7%,wt)
LP71	EC/DEC/DMC (1/1/1, wt/wt/wt)	$LiPF_6$ (12.4%,wt)
LP100	EC/PC/DMC (1/1/3,wt/wt/wt)	$LiPF_6$ (11.46%,wt)
LF100	EC/PC/DMC (1/1/3,wt/wt/wt)	LiFSI (13.74%,wt)

Electrolyte samples were placed in a glass dish of about 67 mm in diameter, which itself was laid onto a sample holder in the central axis of this part of the Tewarson system. The dish was weighed before and after the combustion test to check the possible presence of a residue after the combustion process.

The thermal aggression was provided by external heat flux using four infrared heaters of different power. These heaters do not bring any additional fuel source needed to set fire condition that would otherwise interfere with emissions of effluent gases from the sample under testing. The results can then be utilized to set a fire testing condition comparable to real fire environment.

After combustion, fire products are totally captured and mixed with diluting ambient air in the sampling duct, where the gas temperature and the product-air flow rate are measured. The in-situ on-line analysis of the diluted fire products includes the quantification of O_2 (using a paramagnetic analyzer), CO and CO_2 using a non-dispersive infra-red (NDIR) analyzers and a Fourier-transform infra-red (FTIR), soot through optical measurement and total hydrocarbons (THC) by means of a flame ionization detector (FID). An online supplementary FITR apparatus provides additional, quantitative or qualitative, information regarding (toxic) gas release such as CO, CH_2O, HCN, NO_x, and SO_2 or fluorinated species (HF,…) according to calibration processes and available IR spectra databases. The quantification of these gases allows the detailed and accurate determination of both chemical and thermal threats.

3. Results and discussion

3.1. Short summary of the previous studies on carbonated solvents mixture fire behavior

Of the fire parameters deduced from combustion experiments [18] on different linear and cyclic carbonate solvents used in LIBs' electrolytes, the heat released when a given quantity of material is burned, called effective heat of combustion (ΔHc^{ef}), and the rate at which this heat energy is released (heat release rate-HRR), are the most important variables which govern the fire hazard in a given scenario. Linear carbonate solvents, namely, dimethyl carbonate (DMC), diethyl carbonate (DEC) or ethyl methyl carbonate (EMC) show higher HRR and speed of combustion than the cyclic ones (ethylene carbonate (EC), propylene carbonate (PC)) following their ease of ignition indicators (such as flash points). Moreover, the linear and cyclic solvents mixtures HRR profiles exhibit two well distinguishable successive contributions pertaining to the linear then cyclic solvents; modifying the composition of the linear vs. cyclic carbonates significantly changes the magnitude of the peak HRR value of the mixtures. Interestingly, it was also shown that the

flash point of the solvent mixtures is very close to the more volatile linear solvents indicating a non-ideal behavior of solvents mixtures. Besides, the addition of the $LiPF_6$ salt to the solvents mixture was found not to change remarkably its flash point value, likely due to weak molecular interaction between linear carbonate and the salts ions.

Effective heat of combustion values strongly correlate with the theoretical (total) heat of combustion values obtained from purpose-built predictive Boie model [26] and present a linear dependency on O/C ratio. Hence, unlike most of the hydrocarbons, the effective heat of combustion values of both single solvents and their mixtures can be envisaged using predictive models.

In oxygen rich environments, all fire hazard indicators obtained confirmed a combustion process that releases significant energy and reflects completeness of combustion; in such a case, very limited toxicity is observed, as only CO_2 and H_2O are formed. By contrast, oxygen lean conditions led to various levels of incompleteness of combustion according to types of tested organic carbonates, triggering some toxicity issues driven essentially by carbon monoxide and to some extent by formaldehyde, but not departing too much from ordinary combustible materials.

3.2. Influence of adding the $LiPF_6$ and LiFSI salts on calorimetric and kinetic parameters

All the combustion tests have been performed under oxygen rich environment not to damage the combustion chamber quartz tube; indeed, too high HF gas is concentrated in the combustion chamber while performing experiments under oxygen lean environment as a result of reduced inlet air flow rates.

Moreover, preliminary tests were conducted with the aim of assessing the effect of the external heat flux level (10, 25 and 40 kW m^{-2}) that is supplied to the combustion chamber by making use of four infrared heaters. The obtained results helped us define the appropriate heat flux level applied during all the combustion tests hereafter reported, at a fixed value of 25 kW m^{-2}; This is the value from which no liquid residue (EC and salt containing) is observed at the end of combustion.

3.2.1. $LiPF_6$-based electrolytes combustion tests

The combustion tests were performed on the electrolytes for which the composition and designation are given in Table 1.

3.2.1.1. Heat release rate (HRR). The heat release rate values have been calculated from production of CO_2, CO and soot (CDG calorimetry) as well as from O_2 consumption (OC calorimetry) using equation detailed in previous papers [27,28]; Both methods leading to identical and reproducible results.

HRR results (Fig. 1) of the solvents mixtures and the corresponding $LiPF_6$-based electrolytes show quite similar profiles which denote that the salt does not drastically affect the solvents blends fire behavior; the salt increases the time of combustion (for instance 710 s for LP40 *vs.* 546 s for EC/DEC). This may be explained by the lithium cations desolvation and/or PF_6^- decomposition processes [29–31], both being endothermic.

3.2.1.2. Effective heat of combustion (ΔHc^{ef}). The effective heat of combustion values given in Fig. 2 and Table 2 are calculated by integrating the aforementioned HRR curves and compared with that of solvents blends reported in previous publication [18]. These

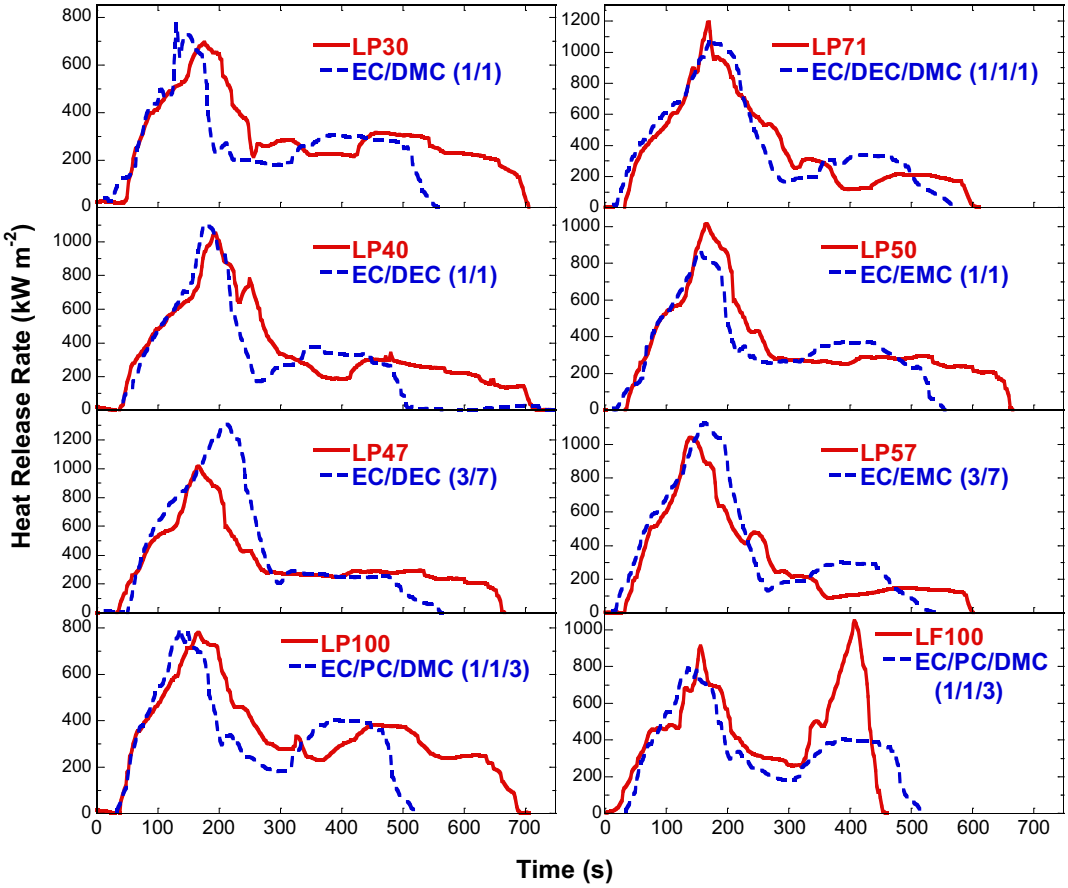

Fig. 1. HRR profiles of tested electrolytes and their corresponding solvents mixtures.

values are taken as averages of triplicate determinations and are reported as kJ per gram of solvents mixture.

Electrolytes effective heats of combustion are the same as the corresponding solvents blends (for instance ~17.09 kJ g^{-1} of solvent for LP40 and 16.99 kJ g^{-1} of solvent for EC/DEC (1/1, wt/wt)), illustrating that $LiPF_6$ salt has negligible effect on the value of combustion energy of electrolytes. This could be explained by the fact that the phosphorus in $LiPF_6$ is already in its maximum oxidation state (P^{V+}). Besides, our preliminary combustion test on $LiPF_6$ salt alone has further confirmed the incombustibility of the salt.

As emphasized in the previous publication, these effective heat of combustion values match well with those predicted from the Boie model; the ratio between both values is nearly 100% (Table 2 and Fig. 2). As a reminder, the predictive equation used is:

$$\Delta Hc\ (kJ\ g^{-1}) = 33.800C + 144.153H - 18.019O \quad (1)$$

where C, H and O are the mass fractions of carbon, hydrogen and oxygen in the burning electrolyte. The effective heat of combustion of electrolytes varies according to oxygen to carbon ratio (O/C) of the electrolytes solvents and based on this, LP30, which has the highest O/C value, presents the lowest heat of combustion and LP47, which has the lowest O/C ratio, possesses the highest energy amid the tested electrolytes.

In summary, from all the combustion tests performed on electrolytes under oxygen rich environment, we infer that the addition of $LiPF_6$ salt does not change the effective heats of combustion obtained for the corresponding solvents mixtures but slightly modifies the HRR profile, increasing the time of combustion. Note that a solid residue is observed at the end of all the combustion tests.

3.2.1.3. Combustion residues XRD and EDX analysis. Whatever the electrolyte tested, the amount of greyish-white colored solid residue left at the end of the combustion is estimated at ~2% of its initial mass (Table 2). From XRD analysis, the residue is composed of LiF (Fig. 3) as crystalline material. Besides, resulting from EDX analysis (Fig. 3 inset), 99.92% at. of the elemental composition of the residue is fluoride with phosphorus traces (<0.1% at.). The mass percentage of residue represents 17% of the $LiPF_6$ mass; this value corresponds to the theoretical ratio m_{LiF}/m_{LiPF6}. This highlights the complete conversion of the salt into LiF and PF_5 according to Reaction (2). The latter, being very reactive towards water vapor always present in fire gases, forms POF_3 [32].

$$LiPF_6(s) \rightarrow LiF(s) + PF_5(g) \quad (2)$$

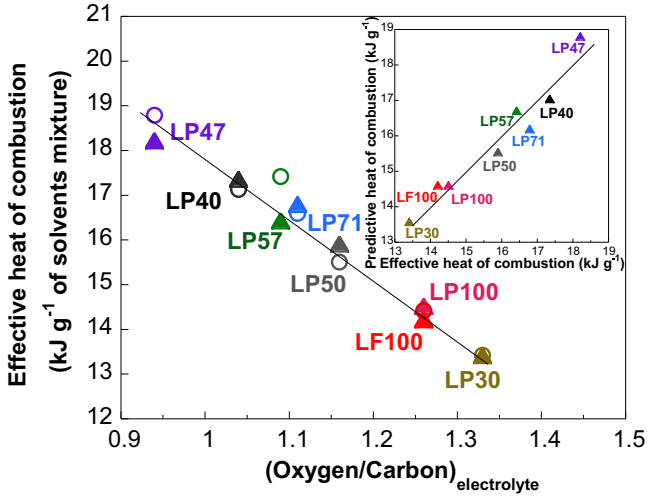

Fig. 2. Correlation between of O/C ratio and effective heat of combustion of electrolytes (per gram of solvents mixture) (▲) and solvents mixtures (○). Inset: correlation between predictive and effective heats of combustion of electrolytes (per gram of solvents mixture).

3.2.2. Comparative investigation of $LiPF_6$ and LiFSI-based electrolytes fire behavior

This study deals with the comparative combustion parameters analysis of EC/PC/3DMC + 1 M $LiPF_6$ and EC/PC/3DMC + 1 M LiFSI-based electrolytes. On-line visual observation of combustion tests showed quite different behaviors, noticeably in the second stage of combustion. In first stage, the combustion behaviors are almost the same, except the time to ignition which is slightly shorter for LiFSI-based electrolyte (~10 *vs.* 38 s). In the second stage, the combustion of LiFSI-based electrolyte was observed to be more explosive and went to extinction in a shorter time.

3.2.2.1. Heat release rate (HRR). Fig. 1 shows HRR profiles of LF100 and LP100 electrolytes and their base solvent mixtures. As can be clearly seen, there is a substantial variation for the two electrolytes for $t > 300$ s, *i.e.* in the second phase of combustion, where LiFSI-based electrolyte presents a quite sharp HRR peak compared to $LiPF_6$ electrolyte. The difference in the HRR evolution is likely to rely on the different salts thermal behavior. Unlike $LiPF_6$ which exhibits an endothermic decomposition path, the thermal decomposition of LiFSI salt is exothermic [16,19].

Conventional liquid pool fires equilibrium regime in steady state is known to come from adjustment of energy radiated from flames to the pool surface which provides the vaporization energy in the case of conventional liquid. This re-radiation effect account for some 2–5% of overall radiated energy [33] in large pools and determine steady-state combustion speed, due to isotropy of radiation transfer. In case of extra-energy developed in the liquid phase by decomposition, this may lead to sharp but transient increase of overall rate of heat release, as energy is more efficiently transferred to the remaining liquid. This type of specific behavior of some substances was already evidenced in previous work on organophosphorous pesticides like chlormephos containing the very reactive –(P═S) chemical bonding [34].

3.2.2.2. Effective heat of combustion (ΔHc^{ef}). Table 2 and Fig. 2 displays the effective heat of combustion of LP100 and LF100 electrolytes and their EC/PC/3DMC solvents mixture. $LiPF_6$-based electrolyte gives similar value as the solvent mixture whereas LiFSI-based electrolyte shows slightly lower value which seems in accordance with the carbon found as residue as discussed hereafter.

Thus, the salts seem again not to have significant added contribution towards the effective heat of combustion and this is not an unanticipated result because, as P^{V+} in case of $LiPF_6$, the sulfur in LiFSI is in its maximum positive oxidation state, S^{VI+}.

3.2.2.3. XRD and EDX analysis of residues. As already stated, the residues for $LiPF_6$-based electrolytes were found to be ~2%wt. (greyish-white color) and their chemical nature determined by XRD and EDX analyses was revealed to be LiF.

LiFSI-based electrolytes combustion leaves ~5%wt. of residues of black colour. XRD diagram revealed the presence of LiF and Li_2SO_4 and some non-assigned peaks (Fig. 3). EDX analysis revealed the presence of carbon (26% at.), nitrogen (12% at.), oxygen (38% at.), fluorine (15% at.) and sulfur (9 % at.). The presence of carbon element is in line with the colour of the residue and is due to incomplete combustion of solvent; this can be explained by the LiFSI presence related 2nd phase combustion reaction suddenness.

Table 2
Comparison of thermal parameters and quantification of toxic effluents released from burning various $LiPF_6$ and LiFSI-based electrolytes.

	LP30	LP40	LP47	LP50	LP57	LP71	LP100	LF100
Initial mass (g)	61.4	58.95	48.02	60.1	47.3	55.35	64.7	61.2
Residue (wt. %)	1.95	1.87	2.29	2.0	2.8	2.17	2.0	5.0
Ease of ignition (s)								
Time to ignition (TTI)	40	30	28	34	26	30	38	10
Time of combustion	676	682	572	638	576	575	695	460
Heat of combustion (kJ)								
Integrated HRR	726	896	760	839	678	814	831	750
Measured heat of comb. (/g of elec.)	11.82	15.20	15.83	13.96	14.33	14.7	12.84	12.25
Measured heat of comb. (/g of solv.)	13.41	17.35	18.21	15.90	16.42	16.79	14.51	14.21
Predicted heat of comb. (/g of solv.)	13.57	17.05	18.80	15.55	16.68	16.19	14.60	14.60
Energy conversion efficiency (%)	98.8	100	96.9	100	98.4	100	99.4	97.3
Product yields (mg gas/g of elect.)[c]								
CO_2	1241	1562	1469	1431	1355	1405	1285	1308
CO	5.5	12.2	16.8	9.2	10.6	9.7	7.6	1.9
HCOH	0.4	0.8	0.4	0.6	0.9	0.7	0.9	0.9
CH_4	–	0.1	0.1	–	–	0.1	–	–
C_2H_4	0.1	–	1.8	0.1	0.1	–	1.6	–
C_2H_2	0.8	0.9	–	0.4	2.9	0.2	–	0.8
THC	6.8	3.3	2.1	1.1	1.6	6.9	–	10.0
Soot	13.2	0.8	4.7	3.4	4.8	–	3.5	7.8
HF	52.4	58.0	53.8	59.5	53.8	52.4	58.4	17.6
SiF_4	2.7	5.2	3.2	10.6	2.3	6.5	4.3	–
HF conversion efficiency (HF + SiF_4) (%)	70[a]	76[a]	65[a]	84[a]	66[a]	70[a]	90[a]	60
	58[b]	63[b]	54[b]	70[b]	55[b]	59[b]	76[b]	–
SO_2	–	–	–	–	–	–	–	70.7
Fuel-S to SO_2 conversion efficiency (%)	–	–	–	–	–	–	–	75
HCN	–	–	–	–	–	–	–	0.4
NO	–	–	–	–	–	–	–	3
Fuel-N to N-containing emissions conversion efficiency (HCN + NO) (%)	–	–	–	–	–	–	–	16

[a] On basis of PF_5 and taken into account HF and SiF_4 content values.
[b] On basis of $LiPF_6$ and taken into account HF and SiF_4 content values.
[c] Unless other units are specified in the table.

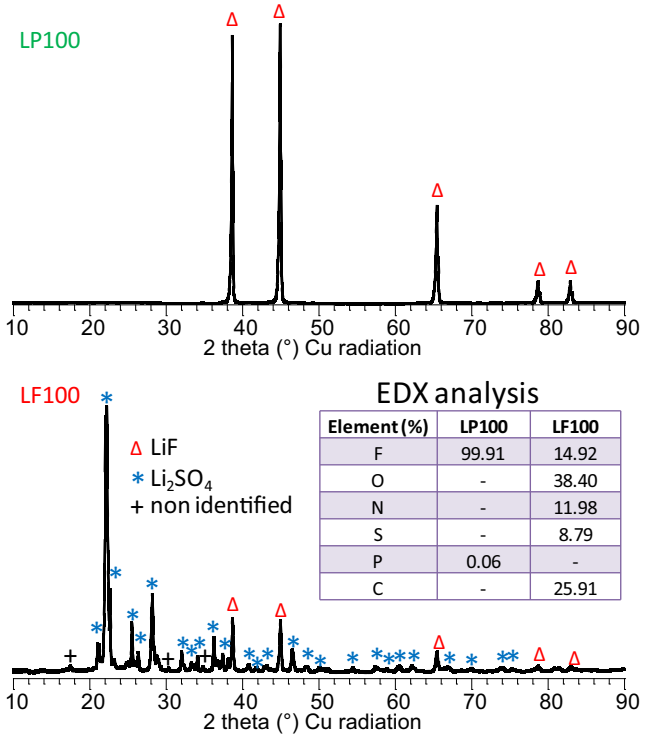

Fig. 3. XRD patterns of LP100 and LF100 electrolyte residues. Inset: EDX analysis.

The O/S ratio is equal to 4.2, which corroborates the XRD result indicating Li_2SO_4 presence. Fluorine is assumed to fully enter the composition of LiF phase as in case of $LiPF_6$ and unfortunately nitrogen could not be assigned. Note that F/N and S/N ratios are equal to 1.25 and 0.75 respectively. In LiFSI salt, these ratios are equal to 2, which indicate that F and S are more easily lost in the gaseous phase. Considering that the total lithium content is retained in residue, we calculated from EDX results the following mass percentages; C (18.6), N (10.7), O (36.8), F (16.9) and S (16.8). The fluorine represents 27% of HF equivalent, the sulfur, 16% of SO_2 equivalent and the nitrogen, 52% of HCN equivalent; these values will be discussed in the following section related to gas emission.

3.3. Gases analysis

Investigations focused on the measurement of soot, CO and CO_2 from (in)complete combustion, unburned hydrocarbons (THC, C_2H_2) and associated oxygenated compounds (such as aldehydes), and salts decomposition products such as HF, SO_2, POF_3, HCN and NO. SiF_4 is also detected, originating from the HF attack on quartz tube and then has to be counted as additional HF in actual scenario of interest. These toxic gas effluents are basically considered as essentially driving an irritant (HF, NO, HCOH and SO_2) or asphyxiant (CO_2, CO, HCN) effect on living targets. More exotic species in fire gases like POF_3 are less well-known but might present more complex systemic effect.

3.3.1. Gases coming from solvents

As shown in Table 2, numerous gases (hydrocarbons, oxygenated compounds) as well as soot coming from solvent molecules are detected in well-ventilated conditions for all tested $LiPF_6$ and

LiFSI-based electrolytes, which differs from the gases released during the solvents mixture burning tests (only CO_2 and H_2O). These results suggest that adding salts into solvent mixtures makes the combustion incomplete. However, except for soot values, these gaseous products are in lower quantity than in case of solvents mixture combustion in oxygen lean environment. As displayed in Fig. 4 in case of LP100, for the example of CO, the gases production starts at the end of the 2nd phase suggesting a kind of pseudo-under ventilated condition; the combustion transits from oxygen rich (first phase with production of CO_2 only) to kind of oxygen lean environment.

Moreover, the amount of CO for $LiPF_6$ is about five times higher than that of LiFSI and $(CO/CO_2)_{LiPF_6}$ to $(CO/CO_2)_{LiFSI}$ molar ratio is 9/2, which implies that the degree of combustion towards completion is less favored in the case of $LiPF_6$ leading to higher potential toxic hazards.

3.3.2. Gases coming from salts

Fig. 4 shows that the release of the HF, SO_2, NO, HCN gases occurs, as CO and other solvents-related gases, at the end of the combustion, in the aforementioned pseudo-under ventilated condition. Besides, it is clearly seen that the HF production span is shorter for LiFSI than $LiPF_6$, which is in compliance with the HRR sketches shown in Fig. 1 for both salts.

3.3.2.1. $LiPF_6$-based electrolytes. The amount of HF released is not negligible (52.4–60.1 mg g^{-1} electrolyte) and, even in well-ventilated conditions, a low quantity of its condensed vapors was found to attack the quartz tube glass (basically composed of SiO_2) with the production of SiF_4 (2.3–10.6 mg g^{-1} electrolyte).

This gas is coming from hydrolysis reactions (Reactions (3) and (4)) yielding also POF_3 then P_2O_5.

$$PF_5 + H_2O \rightarrow POF_3 + 2HF \quad (3)$$

$$2POF_3 + 3H_2O \rightarrow P_2O_5 + 6HF \quad (4)$$

The calculations (Table 2) indicate the corresponding conversion efficiency values vary from 65 to 90%; the conversion efficiencies being calculated considering every fluorine atom (in PF_5) is converted in HF:

$$\text{Conversion efficiency} = m_{\text{detected gas}}/m_{\text{theoretically emitted gas}} * 100 \quad (5)$$

It must be stressed that POF_3 was detected via FTIR technique with the presence of a strong band in the 960–1000 cm^{-1} range and a small one in the 840–900 cm^{-1}. Its quantity could have been evaluated for LP100 to 3.1 mg g^{-1} electrolyte. This low value (corresponding to 2.75% HF equivalent) confirms POF_3 hydrolysis.

3.3.2.2. LiFSI-based electrolyte

3.3.2.2.1. SO_2 gas production. If we consider that total S content in LiFSI turns into SO_2 upon combustion test, we would obtain 94 mg of SO_2 per gram of electrolyte. Hence, the detected SO_2 (70.7 mg g^{-1} electrolyte) leads to a conversion efficiency of 75%. If we add 16% of SO_2 equivalent obtained from residue (in Li_2SO_4), we recover 91%. The relatively high equivalent conversion efficiency for SO_2 could be attributed to the ease of N–S and S–F bond breakage compared to S=O. This is also in agreement with previous findings about the fate of S-containing combustible materials that can be accessed in the open literature [34].

3.3.2.2.2. HF gas production. If we consider that the total F content in LiFSI turns into HF upon combustion test, we would obtain 29 mg of HF per gram of electrolyte. Hence, detected HF value (17.6 mg g^{-1} electrolyte) represents 61% of this theoretical value. If we add 27% of HF equivalent obtained from LiF residue, we recover 88%. Note that the yield of HF in $LiPF_6$-based electrolyte is 3.6 times that of LiFSI.

3.3.2.2.3. HCN and NO gases production. The detected N-containing gases are HCN and NO. The quantity of these gases corresponds to a conversion efficiency in HCN equivalent of 16%. The addition of 52% of HCN equivalent recovered in residue increases the value up to 68%. It must be emphasized that lower conversion efficiencies (few %) are usually expected from the fuel-N (NO_x and HCN) released from organo-nitrogen compounds combustion, which is explained by the high rate of nitrogen recombination into N_2 [35]. The quite surprising elevated value encountered in case of the LiFSI-based electrolyte leads to the idea that rules prevailing for

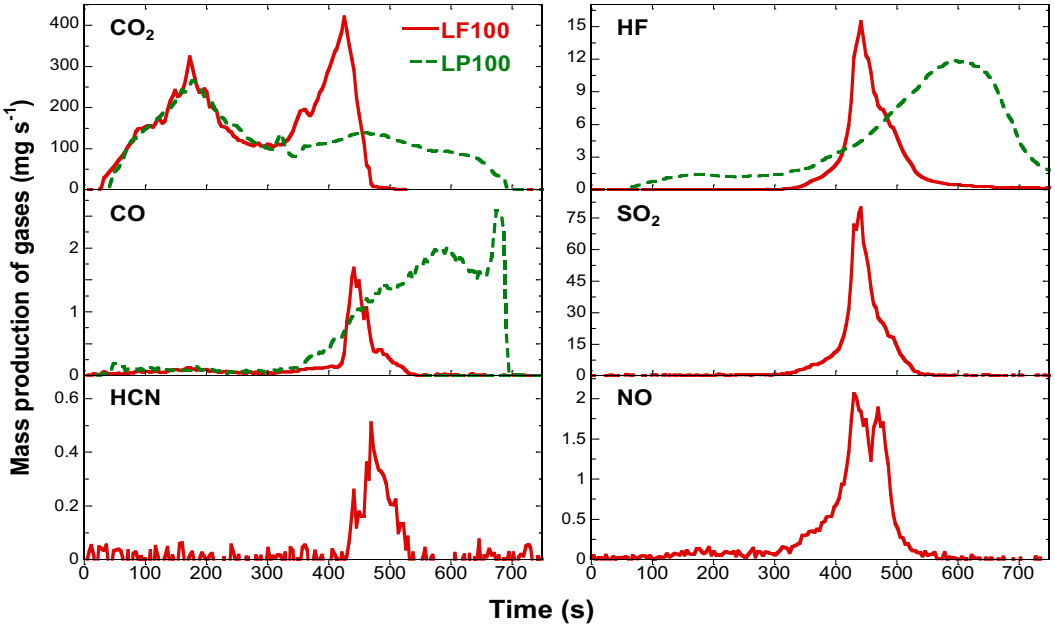

Fig. 4. Yield of toxic gases released during combustion of LP100 and LF100 electrolytes.

conversion efficiency of harmful elements as N, S, P, halogens… encountered in usual combustibles have to be revisited when combustibles are partially mineralized.

3.3.2.3. Further considerations on HF emissions. Actual HF release from various accidental scenarios that may affect the lithium-ion battery value chain (during manufacturing, storage, transport, integration in battery powered systems, end use, or recycling…) has often been a subject of debate and still justifies more research according to inherent toxicity issues, in particular in the context of emergency response in underground park places. Whereas according to our measurements here, we may conclude that HF release would be of major concern in case of massive open pool fires involving tested electrolytes, some favorable factors as hydrophilicity of HF in gaseous state as well as its high capacity of adsorption or reaction with various media (metals, plastics, glass…) will induced fast partial trapping of HF emissions and limit final transport by fire gases to a given critical target.

3.4. Other parameters potentially influencing electrolyte combustion processes

Apart from chemical nature of combustible materials, degree of ventilation (oxidizing environment) of electrolyte fires is by far the main governing parameter of the fire scenario. This may be affected by situations not studied here, like sudden breakdown of the active material in the cathode that can release up to 15% of the oxygen required to complete oxidation of the electrolyte for NMC type cells (according to P. Roth et al. [36]), or by sudden rupture of battery casing. According to technical choice of the active material, interference with the electrolyte burning process in a given thermal runaway scenario leading to a fire occurrence may be more or less easy (reputed quite difficult with LFP type of active material according to better thermal stability). In practice, trade-offs must be considered with relating battery overall performances in terms of capacity, cyclability and so on, before defining optimal selection of the components for a given application.

In the same way, the contribution of the salt in the fire behavior of the electrolytes may be affected by various additives, another current area of investigation.

3.5. $LiPF_6$ versus LiFSI: any winner at light of the work?

From a fire safety management viewpoint, we did not observe major differences in terms of overall energy releases, but observe some important differences in terms of fire dynamics and relating energy and toxic release profiles that underpin small advantages and sometimes drawbacks for both studied salts, according to parameter considered. As a result, more than designating a winning solution in between the two salts tested, the work provides pertinent information to progress in fire safety engineering and risk assessment of energy storage applications involving tested electrolytes.

4. Conclusion

The effect of $LiPF_6$ and LiFSI salts addition on the combustion-related thermal and chemical profiles of carbonate solvents blends has been explored. Speeds of combustion of linear carbonates reveal higher than their cyclic counterparts in our experiments. This is in agreement with ignition characteristics of test electrolytes (see ease of ignition, Table 2) and observations of neat carbonates fire behavior (as reported by Eshetu et al. [18] and in Section 3.1). Accordingly, HRR profiles of linear/cyclic carbonate blend based electrolytes exhibit two well distinguishable burning phases successively driven by dominant contribution of linear then cyclic carbonate solvent component. Adding the salts brings about a substantial variation for the two electrolytes in the last phase of combustion; $LiPF_6$ slightly extends combustion duration whereas LiFSI entails a shorter and sharper HRR peak. This behavior changes can be assigned to their decomposition pathway, endothermic and exothermic respectively.

Effective heat of combustion values of $LiPF_6$ and LiFSI based carbonate electrolytes are comprised between 11 and 16 kJ per gram of electrolyte (between the LP30 and LP47 values). They can be precisely predicted by making use of Boie Model; favoring cyclic carbonate and linear carbonate with short alkyl chain length.

The trend in the evolution of the mass production of all the detected gases was similar and is predominantly produced near to the end of the combustion phenomena when the reaction ultimately passes from oxygen rich to oxygen lean environment. The results confirm that the toxicity issue resulted from effluent is mainly governed by the nature of the salt. The analysis emphasized the interest of using LiFSI for decreasing HF gases evolution (3.6 times less). However, others toxic gases are produced along with HF as SO_2, CO, NO, HCN, which may enhance the toxicity hazards (cumulative effect). A toxicity hazards assessment in case of scenario of interest is under investigation when integrated into functional battery systems and will be unveiled in a forthcoming paper.

Acknowledgments

This work was supported by the “région de Picardie” and FEDER through the DEGAS Project. We are highly grateful to Fluolyte Corporation for kindly giving LiFSI salt. Provision by SP of FTIR calibration data regarding POF_3 is also gratefully acknowledged.

References

[1] K. Zaghib, P. Charest, A. Guerfi, J. Shim, M. Perrier, K. Striebel, J. Power Sources 134 (2004) 124.
[2] A. Du Pasquier, F. Disma, T. Bowmer, A.S. Gozdz, G. Amatucci, J.M. Tarascon, J. Electrochem. Soc. 145 (1998) 472.
[3] P. Ribière, S. Grugeon, M. Morcrette, S. Boyanov, S. Laruelle, G. Marlair, Energy Environ. Sci. 5 (2012) 5271.
[4] D. Lisbona, T. Snee, Process Saf. Environ. Prot. 89 (2011) 434.
[5] T.M. Bandhauer, S. Garimella, T.F. Fuller, J. Electrochem. Soc. 158 (2011) R1.
[6] J. Wen, Y. Yu, C. Chen, Mater. Express 2 (2012) 197.
[7] D. Fouchard, L. Lechner, Electrochim. Acta 38 (1993) 1193.
[8] T.D. Hatchard, S. Trussler, J.R. Dahn, J. Power Sources 247 (2014) 821.
[9] J.R. Selman, S. Al Hallaj, I. Uchida, Y. Hirano, J. Power Sources 97–8 (2001) 726.
[10] A.B. Lees, Chem. Eng. News 91 (2013) 4.
[11] P.G. Balakrishnan, R. Ramesh, T.P. Kumar, J. Power Sources 155 (2006) 401.
[12] B. Bernstein, Chem. Eng. News 86 (2008) 6.
[13] C.J. Govar, J.A. Banner, Safety Testing of Batteries for Navy Devices Using Lithium Ion Technology, IEEE, New York, 2002.
[14] J. Ciesla, J. Power Sources 18 (1986) 101.
[15] L. Chancelier, A.O. Diallo, C.C. Santini, G. Marlair, T. Gutel, S. Mailley, C. Len, Phys. Chem. Chem. Phys. 16 (2014) 1967.
[16] G.G. Eshetu, S. Grugeon, G. Gachot, D. Mathiron, M. Armand, S. Laruelle, Electrochim. Acta 102 (2013) 133.
[17] G. Gachot, S. Grugeon, G.G. Eshetu, D. Mathiron, P. Ribière, M. Armand, S. Laruelle, Electrochim. Acta 83 (2012) 402.
[18] G.G. Eshetu, S. Grugeon, S. Laruelle, S. Boyanov, A. Lecocq, J.-P. Bertrand, G. Marlair, Phys. Chem. Chem. Phys. 15 (2013) 9145.
[19] H.-B. Han, S.-S. Zhou, D.-J. Zhang, S.-W. Feng, L.-F. Li, K. Liu, W.-F. Feng, J. Nie, H. Li, X.-J. Huang, M. Armand, Z.-B. Zhou, J. Power Sources 196 (2011) 3623.
[20] J. Scheers, E. Jonsson, P. Jacobsson, P. Johansson, Electrochemistry 80 (2012) 18.
[21] F. Kita, A. Kawakami, J. Nie, T. Sonoda, H. Kobayashi, J. Power Sources 68 (1997) 307.
[22] A. Abouimrane, J. Ding, I.J. Davidson, J. Power Sources 189 (2009) 693.
[23] A. Tewarson, R. Pion, Combust. Flame 26 (1976) 85.
[24] A. Tewarson, J. Fire Sci. 10 (1992) 188.
[25] A. Tewarson, Z. Jiang, T. Morikawa, Combust. Flame 95 (1993) 151.
[26] K. Annamalai, W. Ryan, Prog. Energy Combust. Sci. 19 (1993) 383.
[27] H. Biteau, A. Fuentes, G. Marlair, S. Brohez, J.L. Torero, J. Hazard. Mater. 166 (2009) 916.

[28] S. Brohez, C. Delvosalle, G. Marlair, A. Tewarson, J. Fire Sci. 18 (2000) 327.
[29] E. Zinigrad, L. Larush-Asraf, J.S. Gnanaraj, M. Sprecher, D. Aurbach, Thermochim. Acta 438 (2005) 184.
[30] H. Yang, G.V. Zhuang, P.N. Ross, J. Power Sources 161 (2006) 573.
[31] B. Ravdel, K.M. Abraham, R. Gitzendanner, J. DiCarlo, B. Lucht, C. Campion, J. Power Sources 119 (2003) 805.
[32] Petra Andersson, P. Blomqvist, A. Loren, F. Larsson, Investigation of Fire Emissions from Li-ion Batteries, SP Technical Research Institute of Sweden, Boras, Sweden, 2013.
[33] A. Hamins, S. Fischer, T. Kashiwagi, M. Klassen, J. Gore, Combust. Sci. Technol. 97 (1994) 37.
[34] G. Marlair, F. Marliere, S. Desmet, C. Costa, M. Leck, W. Siegried, in: Ind. Fire III Workshop Proc., 1996, p. 93.
[35] G.G. De Soete, E. Croiset, J.-R. Richard, Combust. Flame 117 (1999) 140.
[36] E.P. Roth, C.J. Orendorff, in: The Electric Society Interface, Summer 2012, 2012, pp. 45–49.